Proprioceptive contact force and contact point estimation in a stationary snake robot

Jostein Løwer * **Irja Gravdahl** * **Damiano Varagnolo** *
Øyvind Stavdahl *

* *Department of Engineering Cybernetics, Norwegian University of Science and Technology (NTNU), Trondheim, Norway (Corr.Author email: jostein.lower@ntnu.no)*

Abstract: Measuring contact forces and knowing how and where a robot is interacting with obstacles in its environment is particularly useful for developing physics-based Obstacle-Aided Locomotion strategies for snake robots. The current paradigm for obtaining such measurements is mostly hardware-based, and is achieved through physical sensors that are attached to the outside of the chassis. Since external sensors are subject to wear and tear, it is in general preferrable to estimate external forces using solely sensors that may be hidden within the body of the robot. In this paper we contribute towards devising a method for performing such estimation tasks; more precisely, and building on the work of Liljebäck et. al., we analyze the kinematics of the snake robot systems, and propose a method to estimate contact forces and contact points in a case where the robot remains stationary starting from proprioceptive measurements of constraint forces, accelerations, and force balance equations of a rigid body. The efficacy of the estimators in estimating contact point, contact force and direction is verified experimentally.

1. INTRODUCTION

Snake robots are mechanisms designed to mimic biological snakes, which aspire to inherit the robustness and stability properties of biological snake locomotion. Like their biological counterparts, mechanical snakes move using an array of different propulsion techniques such as lateral undulation, sinus lifting and sidewinding. These gaits are explained well by Ariizumi and Matsuno (2017). In principle this makes snake robots suitable for moving and adapting to some specific unknown and challenging environments such as in rubble following landslides or building collapse. As of yet, this is largely an unrealized potential. Many existing systems for Obstacle-Aided Locomotion (OAL) adapt to the environment in an implicit manner only, with little utilization of mechanical sensor information. In contrast, the present work is part of an effort to achieve efficient, robust and intelligent locomotor behavior by exploiting continually updated information about the geometry and mechanical properties of the robot's immediate environment.

This paper investigates how these robots may acquire such information. We limit the study to planar snake robots, i.e., ones that are intended to navigate on a smooth, two-dimensional surface, potentially with obstacles that constrain the obtainable movements, as shown in Fig. 1. Planar snake robots are configured such that the axes of rotation of all joints are perpendicular to the ground plane. Therefore, they are unable to lift parts of their body off this plane, and thus cannot utilize gaits such as side-winding and sinus lifting. Because of this, planar snake robots rely on either anisotropic friction between their body and the ground plane, or contact with obstacles for propulsion. It can be argued that locomotion based on anisotropic ground friction is a form of OAL on the microscopic level. However, according to tradition we distinguish between the two, and define OAL as locomotion that takes advantage of macroscopic obstacles. This is the type of locomotion of main interest in this paper. Furthermore, general results related to planar OAL also apply to OAL in non-planar snake robots.

On one level, efficient OAL amounts to determining how to actuate the joints of the robot so that the links push against obstacles to efficiently produce propulsive forces in the desired direction. This may involve solving estimation problems such as tactile Simultaneous Localization and Mapping (SLAM) (Durrant-Whyte and Bailey (2006) and locating obstacles of a suitable shape in a suitable location to be useful for propulsion. It typically also involves path planning to ensure that the robot encounters a sufficient number of obstacles to maintain propulsion while navigating the terrain.

Information on how and where the snake robot is in contact with its environment is useful and potentially crucial for robust AOL. In this context, it is desirable to measure contact forces as accurately as possible. To the best of our knowledge, the current paradigm to solve this task is through hardware-based approaches, i.e., through sensors mounted on or close to the exterior of the snake.

However, external force sensors have the disadvantage of being exposed to the environment and are subject to wear-and-tear from the movement of the snake robot.

Liljebäck et al. (2012) proposed an external force estimation method that depends solely on sensors hidden within the body of the snake robot. We will refer to such approaches as *proprioceptive contact force estimation*. The term *proprioception* (also referred to as *kinaesthesia*) represents an organism's sense of self-movement and body position. In vertebrates, this sense is encoded by special groups of sensory neurons in joint and muscle tissue. Most vertebrates also have *cutaneous* (or skin) *mechanoreceptors* allowing them to sense skin touch. Previous attempts at contact force measurement have tried to mimic the function of cutaneous mechanoreceptors using an electromechanical measurement system. The method proposed in this paper attempts to achieve similar results by using a system that is modeled after the vertebrate proprioception.

The recent availability of high-quality and low-cost multi-axis force transducers based on, e.g., piezoelectric elements, strain gauges or Fiber Bragg Grating (FBG) transducers, simplifies internal constraint force measurements. In addition, high precision and low cost accelerometers are becoming accessible with the development of mobile technology and household robotics, such as robotic lawn mowers and vacuum cleaners. These technologies enable investigating whether an alternative and economically favorable soft-sensing solution may outperform previous implementations, both in terms of precision and cost. In this paper we propose a method to estimate the contact force and contact point between a planar snake robot and its environment. The method is verified experimentally for a special case where joint angles are zero and the robot remains stationary. This paper serves as a starting point for further investigation into proprioceptive contact force estimation, particularly when the robot is moving.
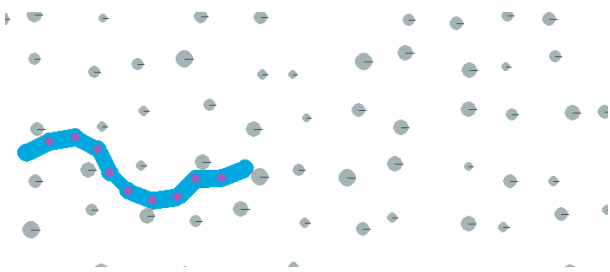

Fig. 1. A simulated planar snake robot consisting of links (blue) and joints (purple) in a cluttered environment of fixed obstacles (gray). To autonomously understand which immediate actuation should be taken to propel oneself forward, and to autonomously plan the trajectory to make sure to be always in contact with enough obstacles to propel in the desired direction, the snake robot must be capable of sensing the surrounding environment and its properties.

2. NOTATION

To increase the readability of the remainder of this document, we present some of the used notation by means of the sketch in Figure 2 and its caption.

To complement this figure, we consider that a generic planar snake robot consists of N links connected by $N_j = N - 1$ joints whose axes are oriented in the same direction. The robot exists in a world coordinate frame (x_0, y_0). Each link of the robot has its own link local coordinate frame (x_i, y_i) where i is the link number. For the remainder of this paper, an integer superscript will denote the reference frame of the variable, and a subscript denotes the link index, e.g., $\ddot{r}_{i-1}^i$ denotes the acceleration of link $i - 1$ in the link local frame of i. The local frames are oriented such that the x-axis forms a line between the axis of joint i and joint $i - 1$, and the y-axis is pointing in the left transversal direction. The tail link of the robot is indexed as link 1 and the head is link N. The link angle of link i, θ_i for $i \in [1 \ldots N]$, is defined as the angle between the global axis x^0 and the local axis x^i. The angle of the ith joint is denoted as ϕ_i for $i \in [1 \ldots N_J]$. In the local frames, forces and torques can be schematized as in Figure 2. The relation between the link angles and the joint angles is finally given by

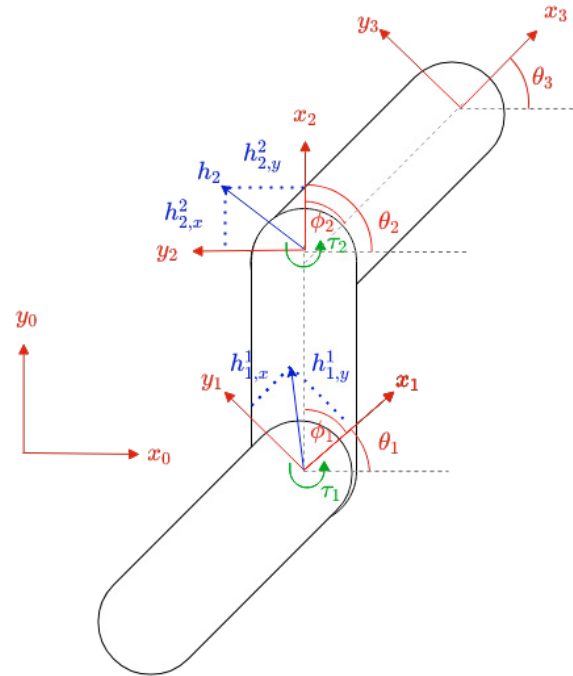$$\phi_i = \theta_{i+1} - \theta_i. \qquad (1)$$

Fig. 2. The kinematics of a simple 3-link planar snake robot as seen from above. The constraint forces h_i^i (blue) are resolved in their link-local frames (red vectors). The link angles θ_i and joint angles ϕ_i (red) relate the orientation of the link-local frames. The link torque τ_i (green) is the control input of the snake robot.

3. PREVIOUS WORK

Existing technologies for measuring contact forces in snake robots can be roughly divided into two categories: discrete and continuous. For example, the systems proposed by Owen (1994); Bayraktaroglu (2009) use discrete contact switches, and are therefore more concerned with contact force detection rather than measurement. The systems implemented by Chen et al. (2008), Transeth et al. (2007),

Fjerdingen et al. (2008), and Taal et al. (2009) instead measure contact forces on a continuous scale.

Common to all of these designs is the placement of force sensors on the outside of the snake robot, directly in between the robot body and the objects it is interacting with, or between the robot chassis and its outer shell.

In more detail, the technology developed by Taal et al. (2009) is an optics based system. Every link of the snake robot is suspended by means of elastic springs within a cage. As the robot comes into contact with an obstacle, the link inside the cage gets displaced. This displacement is then measured using optical range sensors. Given information on the elastic coefficients and disposition of the springs, the measured displacement may then be converted into an estimate of the contact force.

Kulko, a snake robot designed by Liljebäck et al. (2011), implements a system which is similar in principle to the one developed by Taal et al. (2009). In this case each link is covered by a hollow spherical shell attached to the main body through an array of Force-Sensing Resistors (FSR). As the shell collides with obstacles, the resistance of the FSRs under the shell will change as a non-linear function of the contact force. This approach was also examined by Liljeback et al. (2006) and Fjerdingen et al. (2008). Chen et al. (2008) use the same principle to measure contact forces in their wheeled snake robot.

Gonzalez-Gomez et al. (2010) outlines a capacitive contact force measurement system where the sensors can be wrapped around each link. While the primary element for force measurement is different, the approach is similar to the FSR based systems in practice.

Using contact switches as a means of contact force detection is robust, but only provides a binary representation of the contact force (i.e., contact or no contact). In contrast, optical, capacitive or resistive force sensors enables measurement of the contact force on a continuous scale. These sensing techniques rely on material deformation to produce measurements. This translates into a trade-off between material stiffness and sensor sensitivity. Using materials that deform easily increases sensitivity, but might also make the exterior of the robot less robust as all forces to be measured must somehow be relayed from the environment to the robot chassis through the elastic element. This is undesirable, as a snake robot potentially relies on forceful contact between its exterior and the terrain to produce propulsion.

4. A MATHEMATICAL MODEL OF THE PROPRIOCEPTIVE CONTACT FORCE ESTIMATION SYSTEM

Towards the goal of devising the force estimator discussed in the introduction, we derive some considerations on the proprioceptive contact force sensing possibilities starting from the force balance equations of a rigid body. The equations are then utilized in the next sections to derive the proposed estimators. To do so we build on the kinematics and notation defined by Liljebäck Liljebäck et al. (2012).

Ideally, and as illustrated in Figure 2 (middle link with $i = 2$), a link in a snake robot is only affected by three forces:

(1) h_i, the constraint force between link i and link $i+1$ through joint i;
(2) h_{i-1}, the constraint force between link i and link $i-1$ through joint $i-1$;
(3) $f_{c,i}$, the sum of any external forces from the environment acting on the link (not shown in the figure).

Given this assumption, the force balance for a single link can be described as

$$m_i \ddot{r}_i = h_i - h_{i-1} + f_{c,i} \qquad (2)$$

where m_i is the mass of link i and $\ddot{r}_i$ is the acceleration of this link's center of mass, respectively. The goal of the proprioceptive contact force measurement system is to effectively measure $f_{c,i}$ without the use of external contact force sensors. Assuming that the acceleration $\ddot{r}_i$, mass m_i and constraint forces h_i and h_{i-1} can be measured, the contact force $f_{c,i}$ can be calculated as

$$f_{c,i} = h_{i-1} - h_i + m_i \ddot{r}_i. \qquad (3)$$

Thus, by using the proprioceptive measurement of constraint forces and acceleration, it is possible to produce an estimate of the contact forces without the use of external sensors. To reach a form for the equations in (3) that is more suited for software implementation, it is necessary to derive equations for the kinematics of a planar snake robot. We now expand on (3) as defined in Liljebäck et al. (2012).

Define then the constraint force h_i^i as the force from link $i + 1$ acting on link i through joint i resolved in the local frame of link i. To resolve such a constraint force vector in the link local frame of link i, the most natural choice would be to embed a force transducer located in link i measuring the constraint forces between link i and link $i + 1$ directly.

All measurements must be referred to the same reference frame for (3) to be valid, but each constraint force h_i is originally resolved in its link local frame i. To resolve this, we introduce the rotation matrices $\mathbf{R}_{i-1}^i = \mathbf{R}_{\phi,i-1} \in \mathbb{SO}(2)$ which rotates a vector from frame $i - 1$ to frame i, using the joint angle ϕ_{i-1}. By applying these rotation matrices, we can then redefine (3) as

$$f_{c,i}^i = \mathbf{R}_{\phi,i-1} h_{i-1}^{i-1} - h_i^i + m_i \mathbf{R}_0^i \ddot{r}_i^0, \qquad (4)$$

which produces the contact force on link i, $f_{c,i}^i$, resolved in its own link local frame. The product $\mathbf{R}_0^i \ddot{r}_i^0$ can be interpreted as the global acceleration of the link's center of mass, rotated to the link local coordinate frame. The contact force $f_{c,i}$ is the vector sum of the friction force between the environment and the link $f_{f,i}$ and the normal force $f_{n,i}$ so that

$$f_{c,i} = \begin{bmatrix} f_{f,i} & f_{n,i} \end{bmatrix}^T \qquad (5)$$

as shown in Figure 3. The normal force $f_{n,i}$ can be obtained through vector decomposition as $f_{f,i}$ and $f_{n,i}$ are orthogonal by definition. Similar to the force balance used in (3), the external torque $\tau_{c,i}$ acting on link i can be found using a torque balance

$$\tau_{c,i} = \tau_{i-1} - \tau_i - I_i \ddot{\theta}_i \qquad (6)$$
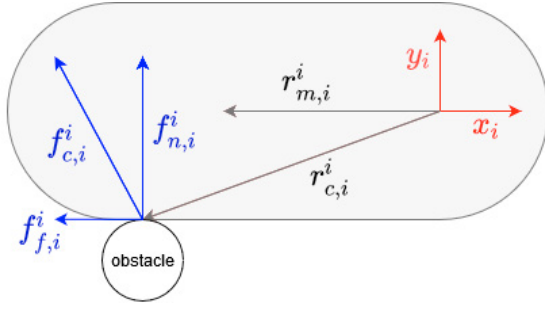
Fig. 3. Schematic representation via a single "pill-shaped" snake robot link of how the link may be in contact with a fixed obstacle.

where I_i is the rotational inertia of link i around the link's center of mass. Assuming that the external torque is caused by the external force $f_{c,i}^i$, the external torque can be written as

$$\tau_{c,i} = (r_{c,i} - r_{m,i}) \times f_{c,i} \qquad (7)$$

where $r_{c,i}$ denotes the position of the point-of-contact between the link i and the obstacle, $r_{m,i}$ denotes the position of the center of mass of link i, and the symbol $\times$ denotes the cross product operator.

Fig. 4. A digital render of a 5-link Boa snake robot, with a soda can for scale reference.

We now examine the special case where the robot is almost stationary, the joints are driven towards a joint angle $\phi_i \approx 0$, and there is no friction between the robot, its underlying surface or the obstacle. This configuration allows us to make the assumptions that

$$\mathbf{R}_{\phi,i} \approx \mathbf{I}, \qquad \ddot{r}_i^i \approx 0,$$
$$\ddot{\theta}_i \approx 0, \qquad f_{f,i}^i = 0. \qquad (8)$$

The assumption $\phi_i \approx 0$ is made to simplify the experimental setup and does not have any significance for the proposed estimators. In a case where $\phi_i \neq 0$, the form or statistical properties of the estimators will not change. Using the assumptions made in (8), on the force balance in (4), meaningful contact force estimates $\widehat{f}_{c,i}^i$ can be computed as

$$\widehat{f}_{c,i}^i = h_i^{i-1} - h_i^i \qquad (9)$$

Using (6) and (7) under the assumptions given in (8), we can estimate the x-component $\widehat{r}_{c,i,x}^i$ of the contact point $r_{c,i}^i$ in the case where the obstacle is in contact with the flat side of link i by

$$\widehat{r}_{c,i,x}^i = \frac{\tau_{i-1} - \tau_i}{\widehat{f}_{n,i}^i} - r_{m,i,x}^i. \qquad (10)$$

Thus, when the normal contact force $\widehat{f}_{n,i} \approx 0$, the signal $\widehat{r}_{c,i,x}^i$ will have a high variance and display a noisy and erratic behavior. Because of this, care must be taken when estimating the position of the contact point when the contact force is low.

5. EXPERIMENTS

A series of 3 experiments were carried out to verify the efficacy of the contact estimation system outlined in Section 4. Experiments 1 and 2 are intended to verify the contact force estimator in (9), and experiment 3 is intended to verify the contact point estimator in (10). All experiments were carried out on a prototype Boa snake robot built at NTNU and configured with 5 links. A digital render of the robot can be seen in Figure 4.
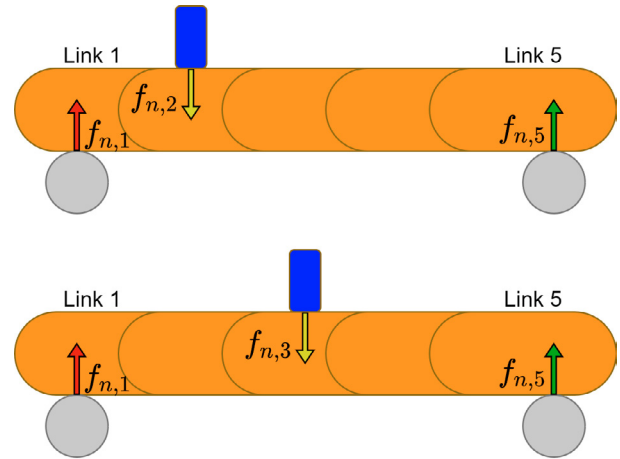

Fig. 5. Experimental setup for Experiment 1 (top) and Experiment 2 (bottom) seen from above. The fixed obstacles are shown in grey, the force transducer in blue and the links of the robot in orange.

The setup of experiment 1 and 2 is shown in Figure 5 as seen from above and with the robot's forward direction to the right. Fixed obstacles were placed on the right-hand side of links 1 and 5. A force transducer (*HBM Z6FC3/20KG*) was used to apply an external normal force to link 2, pushing the robot into the obstacles. The joints of the robot were set to drive towards $\phi_i = 0$ using a PID controller. The force transducers in the joints of the snake robot are of the brand *ME-Messysteme K3D40-50N*. The applied force $f_{n,2}$, and the resulting contact force estimates $\widehat{f}_{n,1}$, $\widehat{f}_{n,2}$ and $\widehat{f}_{n,5}$ are shown in Figure 6. Experiment 2 is similar to Experiment 1 except that the external force is applied to link 3. The applied force $f_{n,3}$, and the resulting contact force estimates $\widehat{f}_{n,1}$, $\widehat{f}_{n,2}$ and $\widehat{f}_{n,5}$ for Experiment 2 are shown in Figure 7.

Experiment 3 is similar in setup to Experiment 1, but the external force is specifically applied at $r_{c,2,x} = -0.085m$. The position of the mass center is known to be $r_{m,i,x} = -0.035m$ for the links of the robot.
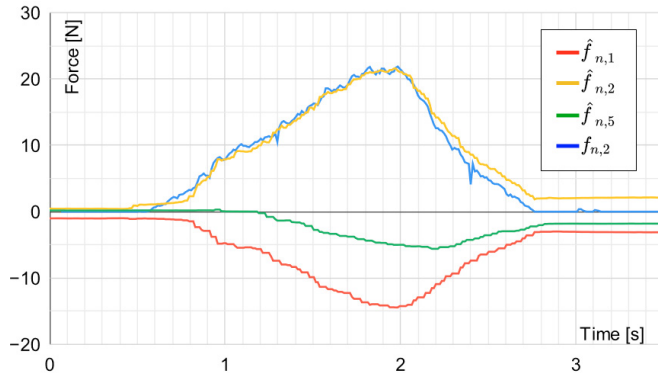

Fig. 6. Estimated contact forces computed from the measurements collected while running Experiment 1.
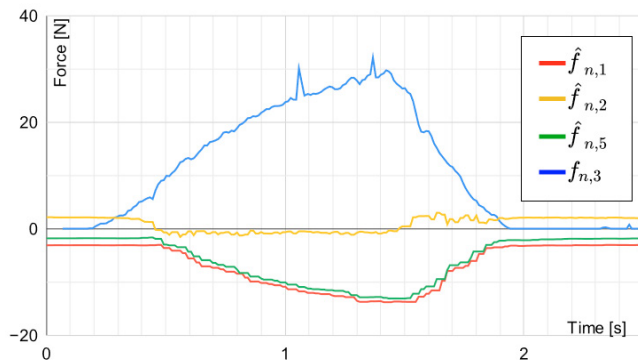

Fig. 7. Estimated contact forces from the measurements collected while running Experiment 2.
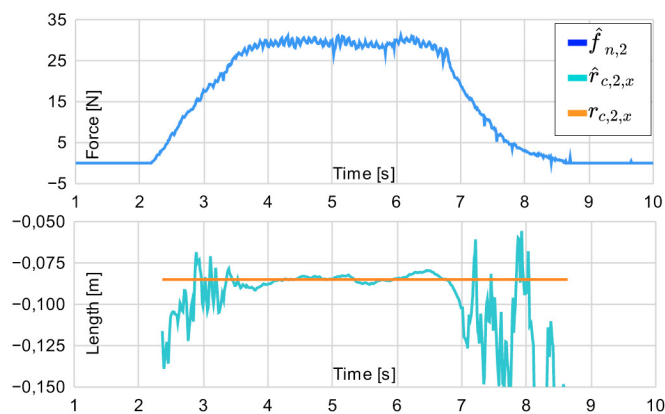

Fig. 8. Applied contact force (upper plot), true contact point position and estimated contact point position (lower plot) for Experiment 3. The estimated contact force $\widehat{r}_{c,2,x}$ is filtered using a 10-tap moving average filter.

6. DISCUSSION

In Figure 6, the estimated contact force $\widehat{f}_{n,2}$ tracks the applied contact force $f_{n,2}$ with little error. Immediately after the applied force is removed at $t = 2.75$, the force estimates $\widehat{f}_{n,1}$, $\widehat{f}_{n,2}$ and $\widehat{f}_{n,5}$ show a stationary error. This is likely due to friction between the snake robot and the ground plane. When the external force is applied, then $|\widehat{f}_{n,1}| > |\widehat{f}_{n,5}|$, which is expected as the point of contact of $f_{n,2}$ is closer to link i than link 5. As the applied force $f_{n,2}$ decreases in the time span $t \in [2, 2.75]$ the estimated contact force $\widehat{f}_{n,2}$ shows an error from the applied contact force $f_{n,2}$. As the force is applied, the joint angles ϕ_i deviate slightly from the target angle of $\phi_i = 0$ as the servos attempt to drive the joint angle towards 0. When the external force is removed, the servos quickly return to $\phi_i = 0$ causing acceleration in the links. This acceleration manifests itself as an error in the contact force estimates through the acceleration term $\ddot{r}_i^i$ in (4). Thus, this is a weakness of the experimental setup rather than the method being studied.

In Figure 7, the estimated contact force for link 2, $\widehat{f}_{n,2}$, is driven towards zero as the external force $f_{n,3}$ is applied to link 3. As an external contact force is applied to the robot, the servos jitter as they attempt to drive towards $\phi = 0$. It is likely that the jitter causes small movements in the body of the snake robot that counteracts the stiction between the robot and the surface.

In Figure 8, the contact point position estimate $\widehat{r}_{c,i,x}$ converges to its true value as the applied contact force converges towards a stationary value $f_{n,2} = 30N$. The estimator performs poorly when the applied contact force is non-constant. This is likely due to two factors: the high variance of $\widehat{r}_{c,i,x}$ when $f_{n,i}$ is sufficiently low and the high noise in τ_i and τ_{i-1} as the servos drive the joints towards $\phi = 0$ to compensate for the applied contact force. While the former is a property of the method being studied, the latter is a weakness of the experimental setup.

7. CONCLUSIONS

We have shown that using a proprioceptive contact force estimation system is a possible strategy for performing meaningful contact force detection and measurement tasks in terrestrial snake robots under semi-static conditions. With this strategy, the proprioceptive systems can be completely hidden within the mechanical structure of the robot, a feature that improves the robustness of the sensing hardware compared to other approaches where the sensors are placed on or near the outside of the robot. The ability to estimate external forces' point of attack is relevant for future tactile SLAM applications.

Physical experiments confirm that the proprioceptive contact force estimators outlined in the paper are promising alternatives to previous methods of measuring contact forces, but refer solely to the case where the robot remains stationary. Further research should be made to develop estimators for contact force and contact point estimation in the case where the robot is in motion, and when the joint angles are non-zero, $\phi_i \neq 0$. The singularity of the contact point (10) as $\widehat{f}_{n,i}^i \to 0$ also requires further investigation to achieve a robust overall system.

REFERENCES

Ariizumi, R. and Matsuno, F. (2017). Dynamic analysis of three snake robot gaits. *IEEE Transactions on Robotics*, 33(5), 1075–1087.

Bayraktaroglu, Z.Y. (2009). Snake-like locomotion: Experimentations with a biologically inspired wheel-less snake robot. *Mechanism and Machine Theory*, 44(3), 591–602.

Chen, T.L.T., Liu, S.H., and Yen, J.Y. (2008). A biomimetic snake-like robot: Sensor based gait control. In *2008 IEEE Workshop on Advanced robotics and Its Social Impacts*, 1–6. IEEE.

Durrant-Whyte, H. and Bailey, T. (2006). Simultaneous localization and mapping: part i. *IEEE Robotics Automation Magazine*, 13(2), 99–110. doi: 10.1109/MRA.2006.1638022.

Fjerdingen, S.A., Mathiassen, J., Schumann-Olsen, H., and Kyrkjebø, E. (2008). Adaptive snake robot locomotion: A benchmarking facility for experiments. In *European Robotics Symposium 2008*, 13–22. Springer.

Gonzalez-Gomez, J., Gonzalez-Quijano, J., Zhang, H., and Abderrahim, M. (2010). Toward the sense of touch in snake modular robots for search and rescue operations. In *Proc. ICRA 2010 Workshop "Modular Robots: State of the Art*, 63–68.

Liljeback, P., Pettersen, K.Y., Stavdahl, Ø., and Gravdahl, J.T. (2011). Snake robot locomotion in environments with obstacles. *IEEE/ASME Transactions on Mechatronics*, 17(6), 1158–1169.

Liljebäck, P., Pettersen, K.Y., Stavdahl, Ø., and Gravdahl, J.T. (2012). *Snake robots: modelling, mechatronics, and control*. Springer Science & Business Media.

Liljeback, P., Stavdahl, O., and Beitnes, A. (2006). Snakefighter-development of a water hydraulic fire fighting snake robot. In *2006 9th International Conference on Control, Automation, Robotics and Vision*, 1–6. IEEE.

Owen, T. (1994). Biologically inspired robots: Snake-like locomotors and manipulators by shigeo hirose oxford university press, oxford, 1993, 220pages, incl. index (£40). *Robotica*, 12(3), 282–282.

Taal, S.R., Yamada, H., and Hirose, S. (2009). 3 axial force sensor for a semi-autonomous snake robot. In *2009 IEEE International Conference on Robotics and Automation*, 4057–4062. IEEE.

Transeth, A.A., Liljeback, P., and Pettersen, K.Y. (2007). Snake robot obstacle aided locomotion: An experimental validation of a non-smooth modeling approach. In *2007 IEEE/RSJ International Conference on Intelligent Robots and Systems*, 2582–2589. IEEE.